Solubilization of Nutraceuticals into Reverse Hexagonal Mesophases†

Idit Amar-Yuli, Abraham Aserin, and Nissim Garti*

Casali Institute of Applied Chemistry, The Institute of Chemistry, The Hebrew University of Jerusalem, Jerusalem 91904, Israel

Received: March 31, 2008; Revised Manuscript Received: May 14, 2008

The solubilization of four bioactive molecules with different polarities, in three reverse hexagonal (H_{II}) systems has been investigated. The three H_{II} systems were a typical reverse hexagonal composed of glycerol monooleate (GMO)/tricaprylin/water and two fluid hexagonal systems containing either 2.75 wt % Transcutol or ethanol as a fourth component. The phase behavior of the liquid crystalline phases in the presence of ascorbic acid, ascorbyl palmitate, D-α-tocopherol and D-α-tocopherol acetate were determined by small-angle X-ray scattering (SAXS) and optical microscopy. Differential scanning calorimetry (DSC) and Fourier-transform infrared (FT-IR) techniques were utilized to follow modifications in the thermal behavior and in the vibrations of different functional groups upon solubilizing the bioactive molecules. The nature of each guest molecule (in both geometry and polarity) together with the different H_{II} structures (typical and fluids) determined the corresponding phase behavior, swelling or structural transformations and its location in the H_{II} structures. Ascorbic acid was found to act as a chaotropic guest molecule, localized in the water-rich core and at the interface. The AP was also a chaotropic guest molecule with its head located in the vicinity of the GMO headgroup while its tail embedded close to the surfactant tail. D-α-tocopherol and D-α-tocopherol acetate were incorporated between the GMO tails; however, the D-α-tocopherol was located closer to the interface. Once Transcutol or ethanol was present and upon guest molecule incorporation, partial migration was detected.

Introduction

The administration of lipophilic/hydrophilic drugs and nutraceuticals is often problematic due to their low water/oil solubility. In order to deliver a therapeutic dose, formulations containing solubilizing agents and/or formulations with a high dissolution rate are necessary.[1]

Lyotropic liquid crystalline phases (LLC), with structural resemblance to human membranes with large surface area and high solubilization capacities, can be used to entrap hydrophilic, amphiphilic, as well as lipophilic guest bioactive molecules.[1–3] In recent years, the liquid crystalline phases formed by surfactants/aqueous mixtures have shown the ability to accommodate biologically active molecules such as vitamins and enzymes.[4–10] Since liquid crystalline structures were introduced to the pharmaceutics world, formulations based on these phases containing drugs have been developed and successfully incorporated in the market (e.g., Amphotericin B-Albelcet, AmBisome and benzoporphyrin−Visudyne).[11,12]

Surfactants/aqueous systems are also used as model matrices to mimic biological processes where the phase behavior of lipids plays a mediating role. The hydrophilic/hydrophobic nature of the guest molecule determines whether the molecule will be preferentially located in the polar aqueous region or in the apolar hydrocarbon domain.[10]

Glycerol monooleate (GMO) is a polar lipid, commonly used as a food emulsifier. When mixed with water it is known to form a wide variety of lyotropic liquid crystalline structures.

In the current research, three extensively studied reverse hexagonal systems[13] were explored as solubilization reservoirs for four bioactive molecules with different polarities. The three H_{II} systems are: the classical reverse hexagonal LLC composed of GMO/tricaprylin (TAG) and water (GMO/TAG weight ratio of 90/10 and 12.5 wt % water), and fluid hexagonal systems containing either 2.75 wt % Transcutol or ethanol as a fourth component (at the expense of the TAG molecules).[13]

The bioactive guest molecules include the following: (1) The first is ascorbic acid, a hydrophilic molecule which, in addition to its well-defined antioxidation properties, can support the myoelectrical activity of the gut (by exerting a neurotrophic effect on VIP-ergic neurons of the ileum).[14] Moreover, ascorbic acid (AA) is mandatory in the hydroxylation of lysine and proline in collagen synthesis and cross-linkage.[15] However, being water-soluble, the sodium salt (ascorbate) has a limited capacity to act at the phospholipid bilayers.[15] (2) Hence we used also a lipophilic derivative of ascorbic acid known as ascorbyl-6-palmitate (AP) as a second guest molecule. AP is an amphiphilic molecule whose structure consists of a hydrophobic palmitic acid side-chain esterified by the polar ascorbic acid molecule at the carbon 6 position, which confers stability and pH independence on the molecule. AP retains the antioxidant properties of AA and accumulates in the carotid body and brain tissues after ingestion.[16,17] (3, 4) The third and fourth bioactive molecules which were solubilized into each of the H_{II} structures were hydrophobic α-tocopherol and α-tocopherol acetate (the α-form showed greater biological effectiveness), which are known to prevent free radical damage in polyunsaturated fatty acids.[18] The tocopherols are also known as membrane-stabilizing agents through their Van der Waals interactions with the membrane phospholipids.[19,20] Vitamin E (VE) is the major natural lipid-soluble antioxidant, present in the cell antioxidant defense system, including the cell membranes of intestine and stomach.[21] Vitamin E acetate (VEA) is widely available in its synthetic form.[22]

* Author to whom correspondence should be addressed. Telephone: 972-2-658-6574/5. Fax: 972-2-652-0262. E-mail: garti@vms.huji.ac.il.

† Part of I.A.-Y.'s Ph.D. dissertation.

10.1021/jp802737k CCC: $40.75
Published on Web 07/30/2008

The nature of the guest molecule, phase behavior, swelling or structural transformations and its location in the different H_{II} structures (typical and fluids) are explored. To study the influence of these bioactive guest molecules and understand their interactions, we have used polarized light microscopy, DSC, SAXS, and ATR FTIR spectroscopy.

Understanding the interactions and implications of these guest molecules and the surfactant/water interactions in their presence is needed not only for their immobilization, but also for their controlled release after administration of the liquid crystalline formulation.[1]

Experimental Section

Materials. Monoolein, GMO, distilled glycerol monooleate that consists of 97.1 wt % monoglyceride and 2.5 wt % diglyceride (acid value 1.2, iodine value 68.0, melting point 37.5 °C, and free glycerol 0.4%) were purchased from Riken (Tokyo, Japan). Tricaprylin (triacylglycerols, TAG; assay 97−98%) was obtained from Sigma Chemical Co. (St. Louis, MO). Ethanol was obtained from Sigma Chemical Co. (St. Louis, MO). Transcutol HP (99.9%) was a kind gift from Gattefossé (Cedex, France). L-(+)-Ascorbic acid, was purchased from Baker Chemical Co. (Phillipsburg, NJ). Ascorbic acid 6-palmitate, was purchased from Sigma Chemical Co. (St. Louis, MO). D-α-tocopherol, Vitamin E 5−96 (contains 1430 international units of vitamin E) was accepted from ADM company (Decatur, IL) and D-α-tocopherol acetate, Vitamin E 6−96, (contains minimum of 960 mg of D-α-tocopherol acetate) was accepted from ADM company (Decatur, IL). Water was double distilled. All ingredients were used without further purification.

Sample Preparation. Hexagonal liquid crystalline samples were formed by mixing all the components while heating to ∼70 °C in sealed tubes under nitrogen (to avoid oxidation of the GMO) for *ca*. 15 min and then cooling to room temperature.

Light Microscopy. The samples were inserted between two glass microscope slides and observed with a Nikon light microscope equipped with cross-polarizers and attached to a video camera and monitor. The samples were analyzed at room temperature.

Small-Angle X-ray Scattering (SAXS). Scattering experiments were performed using Ni-filtered Cu Kα radiation (0.154) from an Elliott rotating anode X-ray generator that operated at 1.2 kW. X-radiation was further monochromated and collimated by a single Franks mirror and a series of slits and height limiters, and measured by a linear position-sensitive detector. The samples were held in 1.5 mm quartz X-ray capillaries inserted into a copper block sample holder. The temperature was maintained at $T \pm 0.5$ °C with a recirculating water bath. The camera constants were calibrated using anhydrous cholesterol. The scattering patterns were desmeared using the Lake procedure implemented in home-written software.[23]

Differential Scanning Calorimetry (DSC). A Mettler Toledo DSC822 measuring model system was used. The DSC measurements were carried out as follows: 5−15 mg hexagonal liquid crystalline samples were weighed, using a Mettler M3 microbalance, in standard 40 μL aluminum pans and immediately sealed by a press. The samples were rapidly cooled in liquid nitrogen from +30 to −40 °C, at a rate of 10 °C min^{-1}. The samples remained at this temperature for 30 min and then were heated at 1 °C min^{-1} to 40 °C. An empty pan was used as a reference. The instrument determined the fusion temperatures of the components and the total heat transferred in any of the observed thermal processes. The enthalpy change associated with each thermal transition was obtained by integrating the area of the relevant DSC peak. DSC temperatures reported here were reproducible to ±0.2 °C.

Attenuated Total Reflectance Fourier Transform Infrared (ATR FTIR). An Alpha model spectrometer, equipped with a single reflection diamond ATR sampling module, manufactured by Bruker (Ettlingen, Germany), was used to record the FT-IR spectra (pure components and/or GMO/TAG/Transcutol or ethanol/water mixture). The spectra were recorded with 50 scans, with spectral resolution of 2 cm^{-1}, at room temperature. The absorbance intensities reported here were reproducible to ±0.005.

Results and Discussion

Solubilization-Dependence of the Reverse Hexagonal Structure by Introducing Hydrophilic and Amphiphilic Molecules. We investigated the impact of ascorbic acid (AA) or ascorbyl palmitate (AP) guest molecules on the macrostructure of the typical (Typ) reverse hexagonal mesophases (H_{II}) formed by the mixture GMO/TAG: 90/10 by weight, with 12.5 wt % water. Up to 5 and 6 wt % AA and AP were solubilized in the well-ordered H_{II} (GMO/TAG/water). For simplicity this system will be termed Typ + AA and Typ + AP, respectively. In the less ordered fluid systems containing 2.75 wt % Transcutol or ethanol lower quantities of AA and AP guest molecules, 4 and 5 wt %, respectively, could be solubilized. We termed these systems Tra + AA, Eth + AA and Tra + AP, Eth + AP, respectively. The three empty systems were initially identified by a light microscope with crossed polarizers. Polarized light microscope images at room temperature of the 3 wt % AA and AP loadings in Typ, Tra, and Eth H_{II} systems are shown in Figure 1a−f. All images containing the solubilizates display birefringent colorful textures that can be attributed to the hexagonal symmetry, although images b, c, e, and f are of fluids of low viscosity samples.

The thermotropic behavior of the GMO/TAG/water, GMO/(TAG + Transcutol)/water and GMO/(TAG + ethanol)/water empty systems (Typ, Tra, and Eth, respectively) was previously studied.[13] Typical DSC thermograms obtained during heating of the three empty H_{II} phases are shown in Figure 2.

During the heating scan of the GMO/TAG/water mixture (Typ, no added solubilizates) from −40 to +40 °C, two major broad endothermic events were detected (thermogram a) with maxima at -2.1 ± 0.2 (peak A) and $+5.9 \pm 0.2$ °C (peak B). Identification of the two peaks was discussed previously.[24,25] Peak A was found to be of melting ice and peak B was attributed to the fusion (melting) of the hydrophobic moieties of the GMO solvated by the TAG.[24,25] It was revealed that the embedment of water binding molecules such as Transcutol or ethanol caused stronger and additional water binding, exhibited in lower melting temperatures (Figure 2).[13] In addition, the hydrophobic melting peak (peak B) was split into three partially overlapping peaks. The melting temperatures of both water and hydrophobic moieties of the GMO in the three H_{II} phases (Typ, Tra, and Eth) empty and loaded with 3 wt % AA or AP guest molecules (Typ + AA, Typ + AP, Tra + AA, Tra + AP, and Eth + AA, Eth + AP), are summarized in Table 1.

The incorporation of 3 wt % molecules of AA or AP composed of five hydrogen-bond acceptor sites (four hydroxyl + one ester group and three hydroxyl + two ester groups, respectively) had a significant effect on the thermal process of the mesophases (Table 1). As expected, an increase in content of the hydrophilic molecule, AA, decreased the water thawing temperature in all three hexagonal systems. However, the water fusion decrease was the most pronounced (by 3 °C) in the Typ

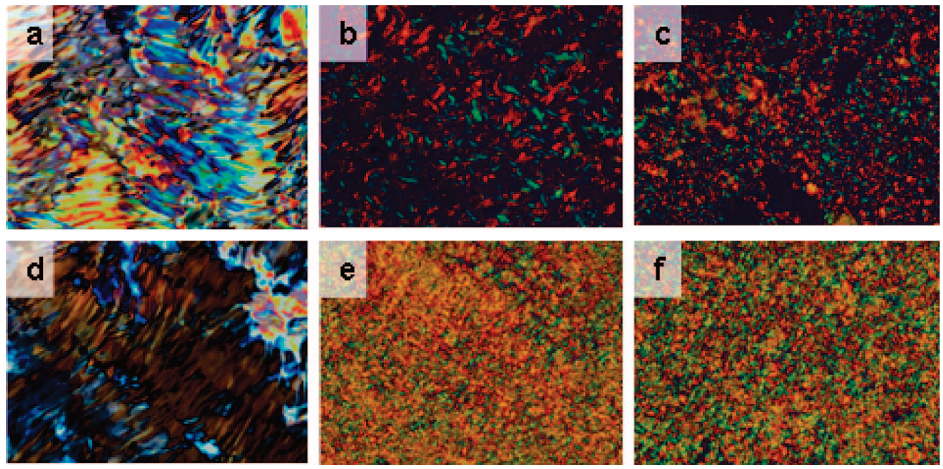

Figure 1. Polarized optical microscope images of typical (GMO/TAG/water, termed Typ) and fluid H_{II} liquid crystal systems (GMO/(TAG + Transcutol or ethanol)/water termed Tra and Eth, respectively), containing 3 wt % AA (a, b, and c, respectively) and 3 wt % AP (d, e, and f). All images were recorded at room temperature.

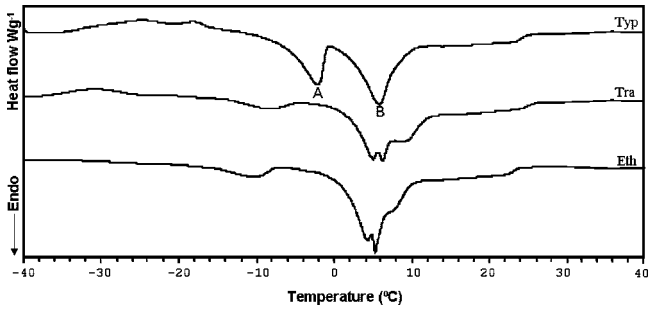

Figure 2. DSC thermograms of GMO/TAG/water mixture (Typ) with two endothermic events at -2.1 ± 0.2 °C (peak A) and 5.9 ± 0.2 °C (peak B), GMO/(TAG + Transcutol)/water mixture (Tra), and GMO/(TAG + ethanol)/water mixture (Eth).

+ AA H_{II} system (Table 1) and least pronounced (by 0.5 °C decrease) in the Tra + AA mixture. AP consists of water-binding sites similar to those of AA except for a single hydroxyl group that transformed into an ester group. AP has similar H-binding capability with water as the AA hence, its accommodation in the three H_{II} phases decreased the water melting temperature, as seen in the presence of the AA molecule (Table 1). On the other hand, it was also detected that the fact that AP consists of a long alkyl tail that solvated by the GMO hydrophobic tails, results in lower tail-melting temperatures in all three hexagonal systems (Table 1).

We calculated the molar ratios of the components (GMO/water/(AA or AP)) in the typical H_{II} phase. At 3 wt % of any of the additives, the mole ratios for GMO/water/AA and GMO/water/AP are ~14/40/1 and 33/93/1, respectively, meaning that one molecule of solubilizate is accommodated within 40 vs 93 molecules of water, respectively. We compared these ratios to those in the fluid hexagonal phases, Tra and Eth, in the GMO/water/AA/(Transcutol or ethanol) and GMO/water/AP/(Transcutol or ethanol), and found them to be ~14/40/1/1 or 14/40/3 and ~33/93/1/2 or ~33/93/1/6, respectively.

We can conclude that although the mole quantity of the two guest molecules, AA and AP, compared to water is extremely small, they induce major competition for water binding with the GMO polar headgroups. The AA and AP molecules interfere with the water interhydrogen bonding; thereby decreasing mainly the ice (water) melting temperature. However, in the presence of additional competitors for water binding, such as Transcutol or ethanol, the function of the AA and AP as water binding agents is less distinct, particularly in the system containing Transcutol. Furthermore, once Transcutol and ethanol were present in the mixture, the contribution of the palmitic tail in solvating the GMO hydrophobic tails is marked, suggesting an additional effect which will be further elucidated by the FTIR. The significant effects of even low guest molecule solubilization is in line with Caboi et al.'s observations when they incorporated vitamin K_1 into a GMO/water mixture.[10] They considered a varying lateral distribution of vitamin K_1 in the lipid bilayer and assumed that the locally higher concentration of the vitamin triggered the phase transitions.[10]

Small angle X-ray scattering (SAXS) was used to identify and characterize the structure of the phases. The SAXS patterns of the three empty mixtures at 25 °C were reported in our previous studies.[13,25] For each mixture three peaks were observed, which were indexed as the (10), (11), and (20) reflections of a 2D H_{II} phase (as can be seen in the Supporting Information).[13] Such a structure is visualized as consisting of cylindrical surfactant micelles arranged in a 2-D hexagonal lattice.[26] It should be noted that in the fluid H_{II} samples, the intensity of the higher order peaks decreased with an increase in temperature, without an increase in the main peak intensity. This was associated with the changing electron density of the compounds upon addition of the glycol (changing the contrast between the solvent and the surfactant).[27] From the three peak positions, we calculated the corresponding mean lattice parameter (a) of the hexagonal structures. The results are summarized in Table 2.

SAXS analysis in the presence of AA and AP molecules (Table 2) reveals an increase in the lattice parameter of the H_{II} phases of all three systems. In the typical H_{II} phase, upon addition of 3 wt % AA a increases by 4.0Å, and in the presence of Transcutol or ethanol a more moderate, yet noticeable, increase is observed (by 1.7−1.5 Å). It should be noted that further increase in the solubilization loads of AA did not further alter the lattice parameter values. In the presence of the AP molecule only a slight increase in a (~1.5 Å) can be detected in all three systems (Table 2).

Hydrophilic guest molecules can be divided into kosmotropic and chaotropic solutes (agents) that are known to exhibit significant impact on the properties of liquid crystalline mesophases by indirect (Hofmeister) interactions with the structures.[28–30] It was found that kosmotropic solutes, such as Transcutol, are likely to be solubilized within the bulk water and be excluded

TABLE 1: Melting Temperatures (°C) of Three H_{II} Systems (Typ, Tra, and Eth) Empty and Loaded with 3 wt % of AA or AP[a]

	melting temperature (°C ± 0.2 °C)								
	Typ H_{II} system			Tra fluid H_{II} system			Eth fluid H_{II} system		
	empty	+AA	+AP	empty	+AA	+AP	empty	+AA	+AP
water (peak A)	−2.1	−5.0	−5.4	−8.4	−8.9	−8.3	−9.9	−12.1	−12.3
tails (peak B)	5.9	5.9	4.8	5.1, 6.5, 9.8	5.4, 6.8	2.9, 5.1	4.3, 5.5, 8.3	4.0, 5.1, 7.6	1.6, 5.0

[a] Typ represents the typical H_{II} system composed of GMO/TAG/water: Tra, GMO/(TAG + Transcutol)/water; Eth, GMO/(TAG + ethanol)/water.

TABLE 2: Lattice Parameters (*a*) of the Three H_{II} Systems (Typ, Tra, and Eth) Empty and Loaded with 3 wt % of AA or AP[a]

	Typ−H_{II} system			Tra−fluid H_{II} system			Eth−fluid H_{II} system		
	empty	+AA	+AP	empty	+AA	+AP	empty	+AA	+AP
a (Å ± 0.5Å)	46.5	51.1	47.9	45.8	47.5	47.3	47.9	47.3	47.2

[a] Typ represents the typical H_{II} system composed of GMO/TAG/water: Tra, GMO/(TAG + Transcutol)/water; Eth, GMO/(TAG + ethanol)/water. The measurements were carried out at 25°C.

from the interfacial areas.[28–30] The kosmotropes interfere with the tetrahedral network of water and, as a result, dehydration of the surfactant polar heads takes place (salting-out effect) and the quantity of interfacial water is decreased. Alternatively, chaotropes tend to destabilize the structure of bulk water and lead to an increase in the area at the water/surfactants interface.[28–30]

Considering DSC outcomes, we can conclude that both AA and AP may increase the hydration level of the headgroups, thereby swelling the cylinders and significantly increasing the lattice parameter. However, the additional tail of the ascorbyl palmitate is effectively solvated by the GMO tail; hence there is a decrease in the extension of the acyl chains, particularly in the Typ + AP H_{II} system. Furthermore, in the fluid system, the Transcutol and ethanol moderate the swelling by causing dehydration of the GMO, thus decreasing parameter *a*.

We conclude that AA performs as a chaotropic agent effectively inducing cylinder swelling, mainly in the absence of the kosmotropic compounds (Transcutol or ethanol). AP exhibits a more moderate chaotropic effect due to its opposite geometric contribution by additional tail volume.

We used FTIR spectroscopy to characterize the microstructure of the H_{II} phases and to spot the guest molecules' location. The FTIR spectrum of the Typ, Tra, and Eth H_{II} phases at 25 °C were reported and discussed in our previous studies.[13,25] Here we compared each system with and without AA or AP (3 wt %) and focused on four major bands depicted in Figure 3, to analyze the conformation of the surfactant molecule and its interaction with water and guest molecules in the different mesophases at 25 °C.

We analyzed the effect of the solubilizates on the hexagonal structure by exploring the bond-vibrations in three regions of

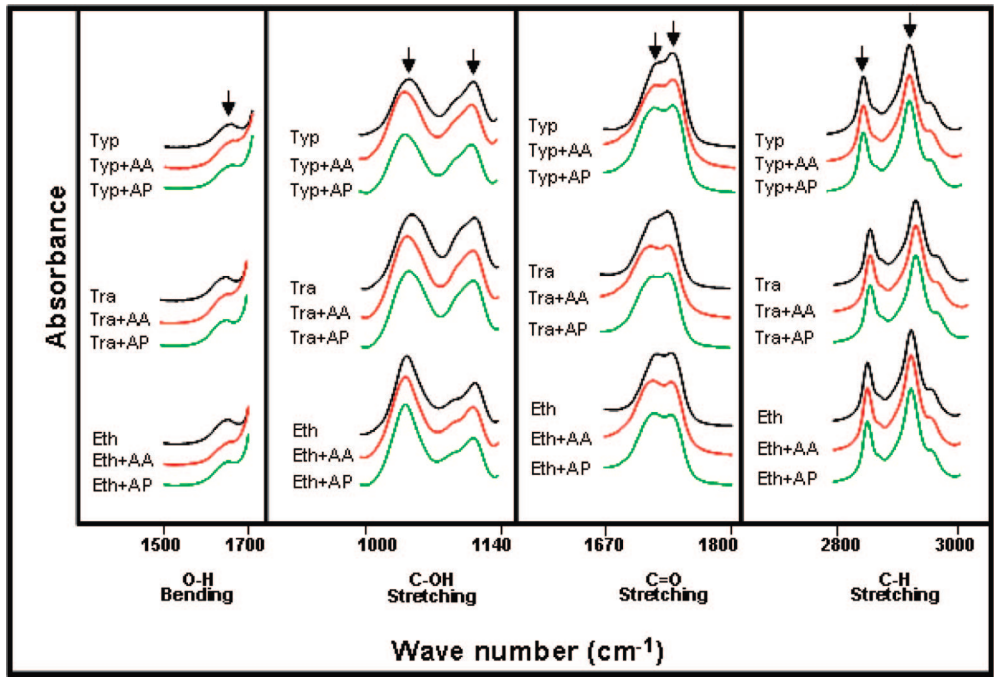

Figure 3. FTIR spectra, at 25 °C, of the three empty H_{II} systems (Typ, Tra, and Eth) and of 3 wt % AA or AP in each system (Typ + AA or AP, Tra + AA or AP, and Eth + AA or AP) in the frequency ranges: (from left to right) O−H bending 1500−1700, C−OH stretching 1000−1140, C═O stretching 1670−1800, and C−H stretching 2800−3000 cm^{-1}. Key: Typ, GMO/TAG/water; Tra, GMO/(TAG + Transcutol)/water; Eth, GMO/(TAG + ethanol)/water.

the mesophase: the water-rich core (the water channels), the water−surfactant interface, and the lipophilic acyl chains.

The H−O−H bending band at ∼1650 cm^{-1} is used to characterize the competitive interactions of the OH of the water with the GMO headgroups and the guest molecules (Figure 3). It is known that the OH bending vibration frequency increases when other moieties (e.g., hydroxyls) compete for the hydrogen bonding.[31,32]

At the interface, three vibrational modes of the GMO headgroups that reflect the interfacial arrangement of the lipid headgroups, are monitored - the stretching of the bonds C−OH (β, ∼1121 cm^{-1}), C−OH (γ, ∼1046 cm^{-1}), and C═O (carbonyl at the α position, 1720−1740 cm^{-1}) (Figure 3).[9,31,33] The carbonyl band consists of two components, one originating from "free" (freely rotating) carbonyl (1740 cm^{-1}) and the second, from intramolecular hydrogen-bonded carbonyl groups (1730 cm^{-1}).[9,33]

Information on the conformational order of the acyl chains is obtained from the stretching modes of the CH_2 segments (ν_{CH_2}). The stretching modes of the GMO methylene groups, shown in Figure 3, are observed at ∼2853 cm^{-1} (symmetric stretching) and at ∼2918 cm^{-1} (antisymmetric stretching).[9,33]

Water-Rich Core. As can be seen in the spectra, solubilizing AA or AP molecules augmented the frequency of the water bending vibrations (Figure 3, first segment). The frequency effect was more pronounced in the Typ and Eth systems (upward shifts of 4 and 2−3 cm^{-1}, respectively) and negligible (1 cm^{-1}) in the Tra mixture (Figure 3, first block). These results are consistent with the DSC behavior that showed a decrease in the water melting temperature with identical tendency (Table 1). The hydrophilic guest molecules distort the water structure and decrease the mean water−water H-bond angle, in the first hydration shell. The H-bond angle is defined by the smallest O···O−H angle formed by two neighboring water molecules, with a linear H bond.[32]

It is known that ionic, polar, and other solutes can perturb the structure of water in different ways with profound consequences for their solubility, hydration thermodynamics, and their association with other solutes.[32] The examined AA and AP guest molecules can be recognized as solutes that destabilize the structure of bulk water (chaotropic effect) and decrease the root-mean-square of H-bond angle, between water molecules.[32] This is achieved mostly by geometric effects in addition to the straightening of the H bonds.

Water−Surfactant Interface. The positions of the C−OH (at the β position on the GMO headgroups, ∼1121 cm^{-1}) and C−OH (γ, ∼1046 cm^{-1}) stretching frequencies were affected by the guest molecules' solubilization in the H_{II} phases (Figure 3). The stronger the hydrogen-bonding between the surfactant and the water (or the guest molecules), the lower the stretching frequency of C-OH group ($\nu_{C\text{-}OH}$). It should be noted that the low $\nu_{C\text{-}OH}$ vibration is attributed to the more hydrated or H-bonded OH group (γ position), hence more changes upon interactions with water or other hydrogen-bond acceptor groups are expected. So far we have detected modifications in the water behavior and only indirectly assumed the corresponding headgroups' action. By focusing on the C-OH stretching vibrations upon addition of AA or AP (constant water concentration, Figure 3), we attempted to identify the moieties along the GMO that exhibit the major modifications, which then will lead to the specific site of the guest molecules in the H_{II} structure.

In the Typ H_{II} phase, upon addition of AA (Typ + AA) the C−OH stretching frequency shifts downward by 4.5 cm^{-1} only in the γ position. However, by solubilizing AP molecules the ν_{C-OH} shift is more moderate, 3 cm^{-1} in the γ position (Figure 3, second block). These results indicate stronger hydrogen-bonding at the hydroxyl groups, mainly in the γ position upon incorporation of AA compared to AP, implying a different solubilization location of the AA and AP within the Typ H_{II} structure. The AA molecule might be located closer to the hydroxyl group in the γ position while AP, due to its alkyl chain, might be located deeper within the surfactant tails, closer to the hydrophobic region. In the Tra H_{II} phase, the peak position (γ) shifts toward a lower wavenumber (5 cm^{-1}, Figure 3, second block) although Transcutol, which tends to dehydrate the hydroxylic groups is present.[13] Considering the DSC results and OH bending vibrations showing only minor changes in the water behavior, it is reasonable to conclude that part of the Transcutol molecules that were H-bonded to the interface are exchanged by the AA or AP solubilizates (1/1 or 0.5 mol ratio of Transcutol/AA or AP). Consequently, more hydrogen bonds between the AA or AP molecules and the OH groups of the GMO are formed. Thus, the kosmotropic additive, Transcutol, is strongly attached to the water molecules and the added chaotropic guest molecules, AA and AP, efficiently interact with the interface hydroxylic groups. Once more, the effect is more pronounced in the γ position upon incorporation of AA compared to AP, showing that AA molecules are located closer to the hydroxyl group in γ position than AP, which is located closer to the hydrophobic region.

On the contrary, in the system containing the hydrotrope, ethanol, the C-OH stretching frequencies shift only slightly downward by 2 cm^{-1} in the γ position upon addition of solely AP molecules. Bearing in mind the strong effect of the water melting temperature upon addition of both guest molecules, we conclude that unlike Transcutol, ethanol stays in the interface and the solubilized additives are localized more in the water-rich core than in the interface. As a result, a stronger effect can be detected in the water-rich core (water behavior) than in the interface which is neutralized by the presence of ethanol (3/1 or 0.5 mol ratio of ethanol/AA or AP). Additionally, based on similar effects in the β and γ positions, we can assume that the ethanol might contribute to the location of the AP molecule and attract it closer to the hydrophilic region.

The changes in the carbonyl bands upon addition of AA or AP are shown in Figure 3 (third block). In the Typ H_{II} phase the major carbonyl band ($\nu_{C=O}$) was detected at 1738 cm^{-1} (free carbonyl band) with an additional lower intensity peak at 1724 cm^{-1} (bonded carbonyl band). The incorporation of AA molecules does not affect the peaks' positions or their intensities. However, addition of AP increases the intensity of the hydrogen bonded carbonyl (lower $\nu_{C=O}$) at the expense of the free carbonyl (by 5%), demonstrating interactions with the carbonyl group. This observation confirms that AP is localized closer to the hydrophobic region than the AA molecule.

In the presence of Transcutol both additives affect the peaks' intensities (increase of 5−10%) and increase the peaks' width at half-height but only the AP molecule slightly increases (by 2 cm^{-1}) the hydrogen bonded carbonyl vibration wavenumber (Figure 3, third block). It is known that the lower $\nu_{C=O}$ is attributed mostly to intramolecular hydrogen bonding.[31,34] Moreover broadening of the C═O stretching band may occur due to a vibrational dephasing mechanism, where the presence of water, for example, would give a broader distribution of vibrational energy levels.[31] This will lead to an increasing perturbation of the C═O stretching mode, which is in line with the experimental observation showing an increase in the broadening of the C═O band with increasing water concentra-

TABLE 3: The Intensities of the CH_2 Wagging Bands (*gg* and *kink*) Normalized to the CH_3 Bending Vibrations of the Three H_{II} Systems (Typ, Tra, and Eth) Empty and of 3 wt % of AP (Typ + AP, Tra + AP, and Eth + AP)[a]

	Typ−H_{II} system		Tra−fluid H_{II} system		Eth−fluid H_{II} system	
	empty	+AP	empty	+AP	empty	+AP
$I_{1354/1378}(gg)$	0.774	0.781	0.740	0.762	0.784	0.802
$I_{1367/1378}(kink)$	0.791	0.791	0.769	0.813	0.780	0.794

[a] Typ represents the typical H_{II} system composed of GMO/TAG/water: Tra, GMO/(TAG + Transcutol)/water; Eth, GMO/(TAG + ethanol)/water.

tion.[31] On the basis of the above observations, we conclude that the accommodation of both additives in the interfacial region perturbs the C═O stretching mode, particularly the amphiphilic AP which breaks fraction of the intramolecular hydrogen bindings (in the GMO molecule) due to its presence.

In the presence of the interface-located ethanol, which assumed to neutralize the effects of AA and AP, indeed only a slight increase in the intensity of the hydrogen bonded carbonyl at the expense of the free carbonyl (by 2−3%), is observed (Figure 3, third block). This effect is consistent with the hydroxyl groups' behavior and demonstrates similar interactions of AA and AP with the carbonyl group. It clearly confirms that the polar moieties of the AA and AP are localized in the same position within the mesophase.

Hydrocarbon Chain Region. In all three systems the methylene peaks are not affected by the incorporation of either AA or AP guest molecules (Figure 3, fourth block). On the other hand, the melting of the GMO fatty chains is influenced by the presence of AP in all the mixtures, as seen from the DSC thermograms. To reconfirm the effect of AP on the mesostructure we followed the CH_2 wagging mode in the IR spectral region of 1330−1400 cm^{-1}. It provides information on the effect of the GMO CH_2 groups that are involved in nonplanar (*gauche*) conformers.[9,35] As a rule, this range of frequencies consists of the *end-gauche* band (*eg*) at ∼1341 cm^{-1}, the double-*gauche* band (*gg*) at ∼1354 cm^{-1}, and the band of *gauche*−*trans*−*gauche* (*kink*) at ∼1367 cm^{-1}. In the spectral region of interest, a band at ∼1378 cm^{-1} also appears, due to the symmetric bending of the end CH_3 group (*umbrella* mode). This band is insensitive to conformation as well as to chain length and its intensity may hence be used as an internal standard with which to normalize the intensity of the conformation-sensitive wagging modes.[9,33,35]

By normalizing the intensities of the three CH_2 wagging bands to the CH_3 bending vibrations, only the *gg* and the *kink* bands (at ∼1354 and ∼1367 cm^{-1}, respectively) show dependence on the solubilized AP (Table 3). In the typical H_{II} phase, where the presence of AP slightly decreased the hydrophobic melting temperature by ∼1 °C, only the double-*gauche* band (*gg*) is shifted (Table 3). However, in the fluid Tra and Eth H_{II} phases, the addition of the amphiphilic AP increases the fractions of both double-*gauche* and *gauche*−*trans*−*gauche* conformers in the GMO tails (Table 3). It should be pointed out that the effect was more distinct in the mixture containing ethanol, which is in line with lower melting points temperatures of the GMO tails observed by DSC.

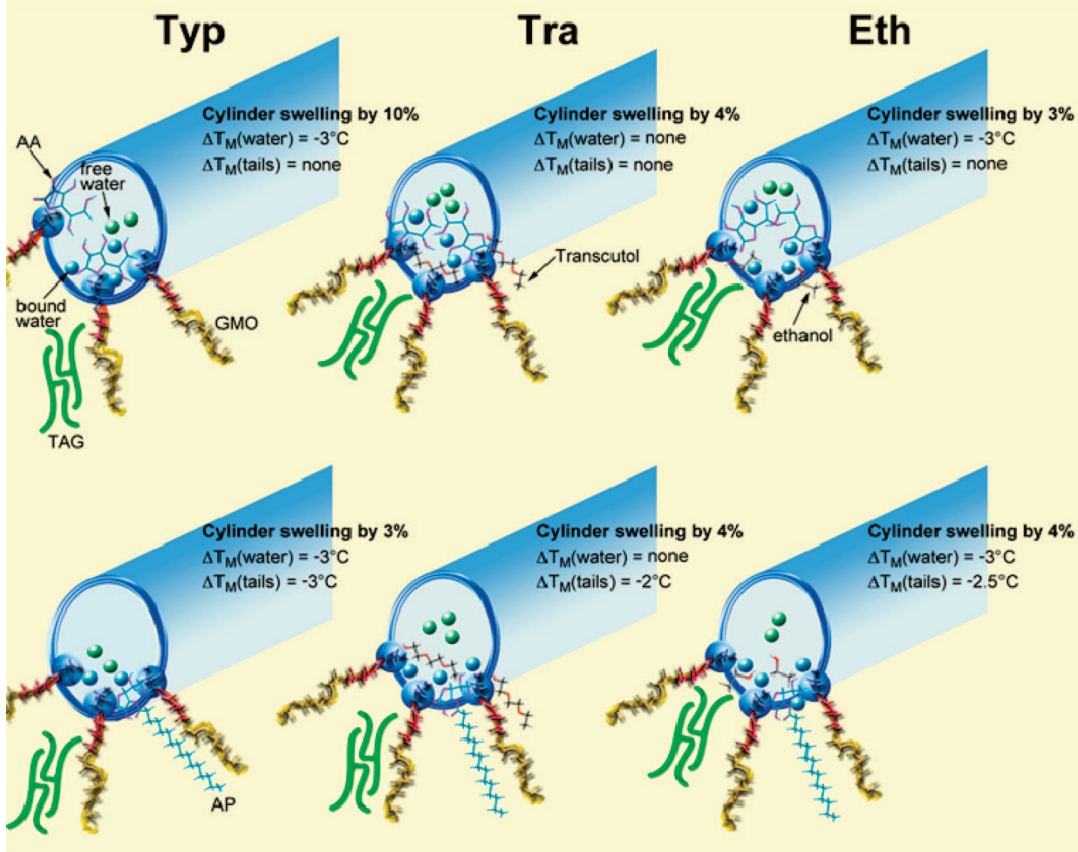

Figure 4. Cartoon illustrating the solubilization location and interactions of AA (upper part) and AP (lower part) in the three H_{II} systems (from left to right) Typ, Tra, and Eth. Three major modifications in the H_{II} properties are indicated: cylinder swelling (%), based on the lattice parameter values, and $\Delta T_{M(water)}$ and $\Delta T_{M(tail)}$: the change in melting temperature of the water and GMO tail, respectively, upon the solubilization process, based on DSC thermograms. It should be noted that the molecular ratio between all the components should not be determined from the image.

The increase in *gauche* conformations results in increased chain disorder and looser acyl chain packing.[33] We conclude that the incorporation of AP in the presence of Transcutol or ethanol increased chain disorder and led to looser acyl chain packing even at very low temperatures (DSC results).

The influence of the AA and AP guest molecules and their location in the three H_{II} phases is summarized by illustration in Figure 4. It was found that in the H_{II} structure, the AA acts as a chaotropic guest molecule, located in the water-rich core and at the interface (Figure 4). Hence, its effect was more pronounced on the water and interface behavior, including cylinder swelling, water fusion temperature and interactions with hydroxyls and carbonyl functional groups.

The AP acts as a chaotropic guest molecule as well, yet it is solubilized at the interface by its polar head while its lipophilic fatty tail is strongly solubilized and embedded within the GMO hydrophobic fatty tail (Figure 4). Hence its presence affected all three regions of the H_{II} structure, the water-rich core, the interface and the hydrophobic tail region. AP decreased water and tail fusion temperatures and interacted with carbonyl and methylene groups.

It was revealed and established that in the typical system and in the presence of ethanol, both AA and AP are solubilized closer to the vicinity of the water than the interface in comparison to their solubilization location if Transcutol was part of the mesostructure. We also learned that the AA and AP induced partial migration of Transcutol from the interface to the hydrophobic region (GMO tail).

The impact of the two solubilizates in both the typical system (Typ) and in that containing ethanol (Eth) was more pronounced on the water behavior than on the interfacial layer and *vice versa* in the presence of Transcutol.

Solubilization-Dependence of the Reverse Hexagonal Structure by Introducing Hydrophobic Guest Molecules. We examined the impact of more lipophilic guest molecules such as D-α-tocopherol (Vitamin E, termed VE) and D-α-tocopherol acetate (VEA) on the macrostructure of the three H_{II} phases. Up to 4 wt % VE and VEA were solubilized in all three systems. Calculating the solubilization capacity on a molar basis yields solubilization loads, 2.5−3.5 times lower than AA or AP. Therefore we reduced the TAG component in the mixture by the corresponding quantities of the lipophilic vitamins up to a complete substitution. Once such mixtures were prepared, the loading capacity of VE or VEA increased and was typical for fluid H_{II} (Typ) systems, 8.5 and 5.8 wt %, respectively.

The polarized light microscope reveals that there are no microscopic noticeable differences between the two empty fluid systems (with Transcutol or ethanol) and those in which VE or VEA were incorporated in all mixtures.

Polarized light microscope images of the Typ and Tra systems containing VE (4 wt %, Figure 5a,b, Typ + VE and Tra + VE, respectively) and VE at the expense of TAG (8.5 and 5.8 wt %, Figure 5c,d, Typ + VE (no TAG) and Tra + VE (no TAG), respectively) at room temperature are shown in Figure 5. All images containing the solubilizates display birefringent and colorful textures that can be attributed to the hexagonal symmetry.[26] However, a few hours after sample preparation, if TAG was not included in the mixture, a lamellar structure was detected, and only after ∼24 h was the hexagonal phase formed. This result suggests that TAG is more efficient than VE or VEA in structuring the H_{II} phase.

DSC measurements reveal that the incorporation of VE or VEA molecules (consisting of two hydrogen-bond acceptor sites—hydroxyl + ether groups and ester + ether groups, respectively) had moderate, yet noticeable, influence on the thermal process of the phases. However, we did not detect any significant differences between the two fluid systems (with Transcutol or ethanol) and the solubilized VE or VEA. The DSC results obtained during heating the Typ and Tra H_{II} phases containing VE (4 wt %, Typ + VE and Tra + VE, respectively) and VE at the expense of TAG (8.5 and 5.8 wt %, Typ + VE (no TAG) and Tra + VE (no TAG), respectively) are summarized in Table 4.

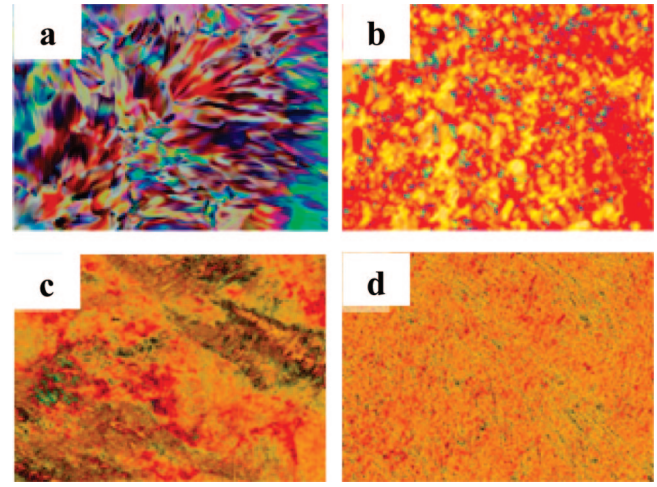

Figure 5. Polarized light microscope images Typ and Tra systems containing of (a, b) 4 wt % VE (Typ + VE, Tra + VE) and (c, d) 8.5 and 5.8 wt % VE at the expense of TAG (Typ + VE and Tra + VE (no TAG), respectively) at room temperature.

Incorporation of the VE molecule together with TAG slightly decreases the water fusion temperature in the typical and fluid H_{II} systems (∼0.8 and 1.8 °C) and promoted the beginning of the GMO chain melting in the fluid system (by ∼1 °C, Table 4, Typ + VE and Tra + VE, respectively). When all the TAG is replaced by VE in the typical H_{II} system, the water fusion temperature is not shifted but the GMO chain melting was postponed to a higher temperature (at ∼12 °C, Table 4, Typ + VE (no TAG)). However, in the fluid system, the water melting point was increased by 1.6 °C, conversely to the hydrophobic chain melting which remained unaltered (Table 4, Tra + VE (no TAG)).

We conclude that the balky hydrophobic part of the vitamin E was not effectively solvated in the GMO hydrophobic tails in comparison to the TAG abilities, resulting in higher melting temperature (Table 4). This conclusion is in line with the formation of a lamellar phase a few hours after replacing the TAG molecules by VE. However, once Transcutol or ethanol is present, the impact of the VE on the thermal process was more distinct in the water behavior than in the hydrophobic region. We interpret the increase in the water fusion temperature as a result of partial migration of Transcutol and ethanol upon incorporation of the bulky VE molecule. This assumption may explain the maintenance of the hydrophobic peak at low temperature although TAG has been replaced by VE molecules.

SAXS analysis in the presence of VE or VEA molecules reveals no significant changes in the lattice parameter of the H_{II} phases of all three systems (±1 Å). Since these two hydrophobic vitamins are expected to be located in the hydrophobic region, they are not expected to modify the lattice parameter.

Utilizing FTIR spectroscopy for characterization of the microstructure of the H_{II} phases on a molecular level, we could find additional information concerning VE and VEA interactions

TABLE 4: Melting Temperatures (°C) of the Typ and Tra H_{II} Systems, with 4 wt % VE (Typ + VE and Tra + VE) and with 8.5 and 5.8 wt % VE, Substituting the TAG Molecules, Respectively[a]

	melting temperature (°C ± 0.2 °C)					
	Typ−H_{II} system			Tra−fluid H_{II} system		
	empty	+VE	+VE (no TAG)	empty	+VE	+VE (no TAG)
water (peak A)	−2.1	−1.3	−2.2	−8.4	−6.6	−6.8
tails (peak B)	5.9	6.0	11.9	5.1, 6.5, 9.8	4.8, 5.4, 9.5	4.9, 7.9, 9.3

[a] Typ represents the typical H_{II} system composed of GMO/TAG/water and Tra represents the fluid GMO/(TAG + Transcutol)/water system.

with the water and GMO. We compared each system with and without VE or VEA (in addition to the TAG molecule and in its absence) and focused on 4 major bands depicted in Figure 6.

Water-Rich Core. Conversely to the impact of the hydrophilic and amphiphilic guest molecules on the water behavior, the hydrophobic additives decrease the frequency of the water bending vibrations (Figure 6, first block). Obviously, it is more pronounced when the TAG is replaced by VE or VEA. In the Typ + VE or VEA (no TAG) and Eth + VE or VEA (no TAG) systems, the O−H bending peaks are shifted to lower frequencies by ∼4 cm^{-1}. In the presence of Transcutol the decrease in the frequency of the water bending vibrations is less pronounced (only by 2 cm^{-1}; Figure 6, Tra + VE or VEA (no TAG)). The hydrophobic guest molecules increase the mean water−water H-bond angle in the first hydration shell.[32] This is primarily a geometric effect since these more lipophilic guest molecules can interact only weakly and nondirectly with water.[32] We conclude that VE and VEA do not protrude into the water structure in comparison to the TAG. These results are consistent with the DSC thermograms that showed an increase in water melting temperature in the presence of VE and VEA (Table 4).

Water−surfactant interface. The incorporation of VE or VEA with and without TAG molecules had no influence on the frequency of the C−OH at the β position on the GMO headgroups (∼1121 cm^{-1}) and C−OH at the γ position (∼1046 cm^{-1}) stretching modes in all three systems (Figure 6, second block). These findings strongly indicate that the hydrophobic guest molecules do not interact with these functional groups, which are placed in the inner water cylinders, as discussed above.

Following the changes deeper in the hydrophobic moiety of the GMO, in the carbonyl group, a more distinct impact can be seen even compared to AP incorporation (Figure 6, third block). The incorporation of VE or VEA that have been substituted for the TAG molecules, affects the peaks' positions and intensities (Figure 6). The intensity of the hydrogen-bonded carbonyl stretching vibrations increases above that of the free carbonyl (by 5−11%, in Typ + VEA and VE (no TAG), respectively). It means that the fraction of the hydrogen-bonded carbonyl is larger than that of the free carbonyl. Moreover, the free carbonyl stretching band is shifted by −3 cm^{-1} in the presence of VE or VEA, revealing that the solubilizates are interacting with the interface (hence indirectly with the water) and their location is adjacent to the interface. On the basis of steric interference considerations it seems that vitamin E is more efficiently incorporated at the interface than vitamin E acetate.

In the presence of Transcutol both solubilizates mainly affect the vibrational peaks' intensities (Figure 6, third block). The Tra + VEA and Tra + VE (no TAG), similarly to the typical H_{II} system, reveal that the intensity of the hydrogen-bonded carbonyl stretching vibrations increases above that of the free

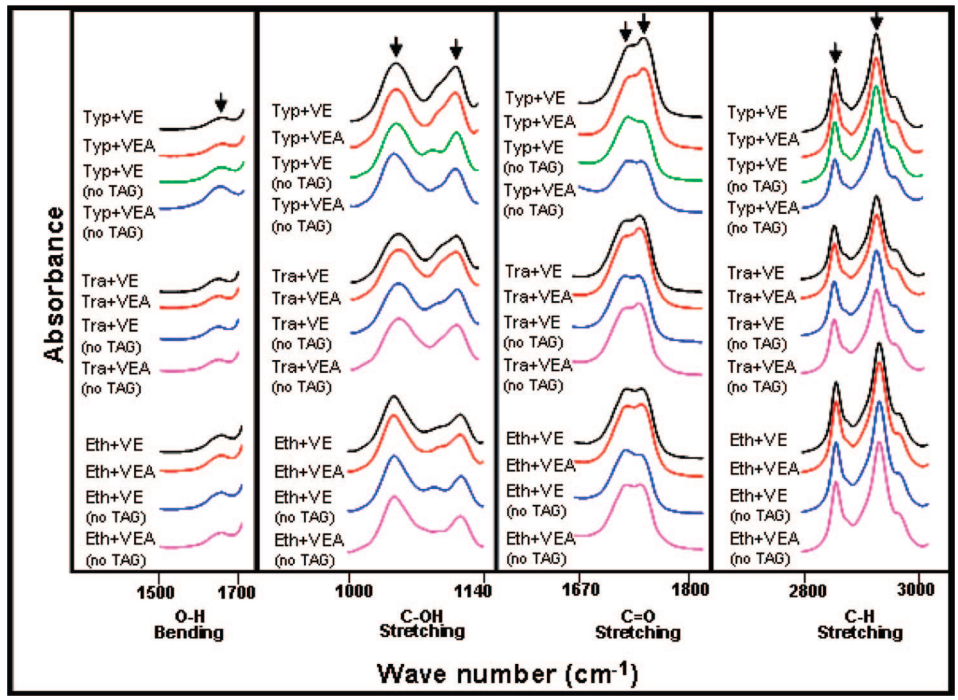

Figure 6. FTIR spectra, at 25 °C, of the three H_{II} systems with 4 wt % of VE and VEA (Typ + VE or VEA, Tra + VE or VEA, and Eth + VE or VEA), and with 8.5 and 5.8 wt % VE and VEA at the expense of TAG (for example: Typ+VE (no TAG)). The frequency ranges are as follows (from left to right): O−H bending 1500−1700, C−OH stretching 1000−1140, C═O stretching 1670−1800, and C−H stretching 2800−3000 cm^{-1}.

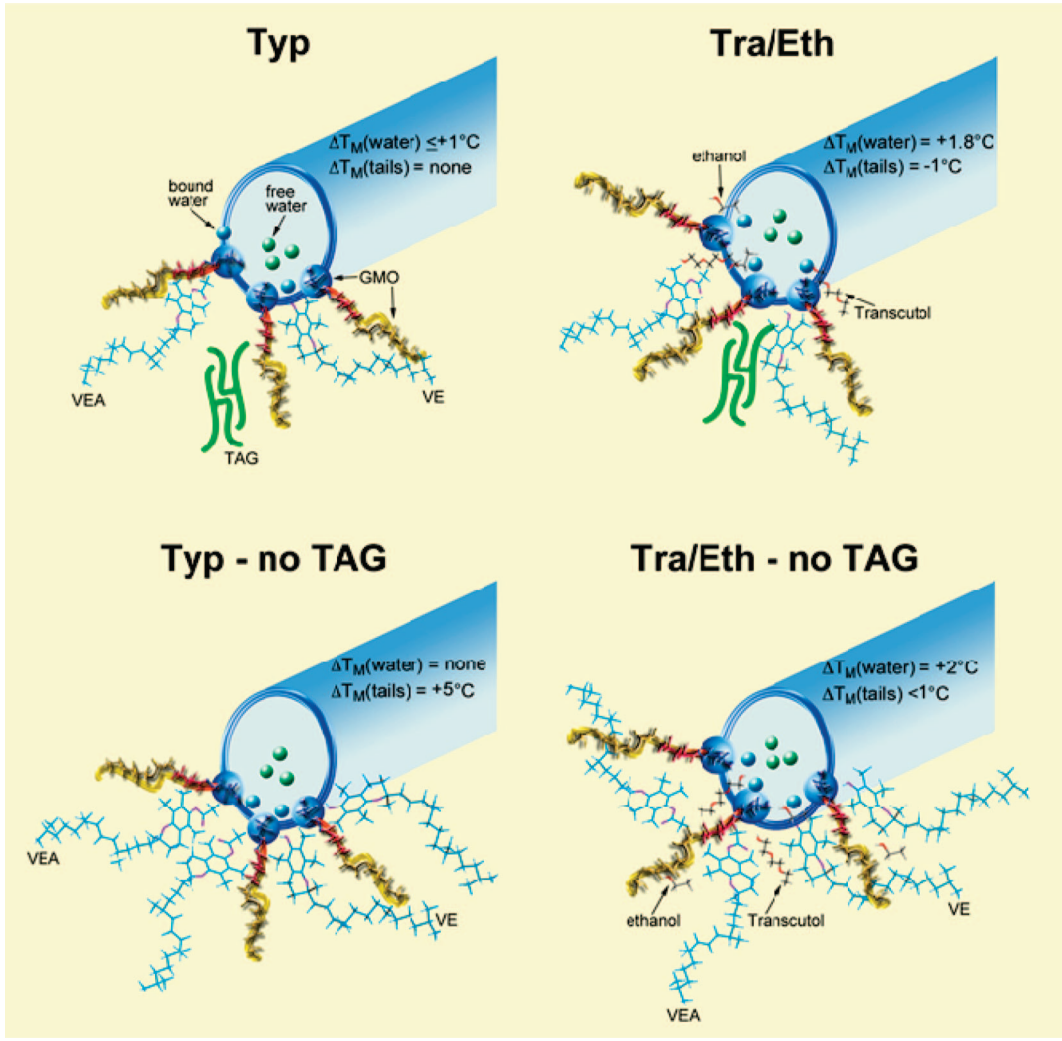

Figure 7. Cartoon illustrating the solubilization location and interactions of VE and VEA in the presence of TAG (upper part) and when replacing the TAG (lower part) in the typical (left) and fluid (right) H_{II} systems. Two major modifications in the H_{II} properties are indicated: $\Delta T_{M(water)}$ and $\Delta T_{M(tail)}$—the change in melting temperature of the water and GMO tail, respectively, upon the solubilization process, based on DSC thermograms. It should be noted that the molecular ratio between all the components should not be determined from the image.

carbonyl (by 4 and 9%, respectively). VE and VEA interactions with the interface increase the hydrogen-bonded carbonyl fraction relative to the free carbonyl. We see again that the more lipophilic VEA (with an ester group instead of a hydroxyl group) is located deeper in the interface than the VE. The overall impact of the addition of VE and VEA in the fluid H_{II} structures is somewhat less pronounced than in the typical one, probably due to the migration of the Transcutol or ethanol.

Hydrocarbon Chain Region. In all three systems the presence of VE or VEA did not affect the methylene peaks' positions (Figure 6, fourth block). However, the intensities of the stretching vibrations of the GMO methylene groups (symmetric and asymmetric stretching) decreased by 7−9 and 21−23%, respectively, only in the typical H_{II} system upon addition of VE and VEA. This result points out that the tails are more tightly packed and are less solvated in the presence of these bulky guest molecules.

These observations can be further reinforced by modifications in the CH_2 wagging vibrations, mainly the double-*gauche* conformations. In all three systems addition of 4 wt % VE or VEA slightly decreases (by 1−2%) the *gg* conformation, suggesting that VE and VEA interfere with the TAG-GMO solvation. Furthermore, replacing all TAG molecules with VE or VEA, results in a decrease of the *gg* conformation fraction by 3 and 6%, respectively, in the fluid H_{II} systems and by 7 and 11% in the typical one. All impacts were more pronounced in the typical H_{II} system, in good agreement with the higher melting temperatures of the GMO tails observed by DSC.

Once more we observe that the balky hydrophobic part of the vitamin E was not efficient in solvating the GMO hydrophobic tails in comparison to the TAG, resulting in a lower *gauche* conformation fraction and higher melting temperature. However, in the presence of either Transcutol or ethanol the impact of these hydrophobic guest molecules was more moderate. We conclude that Transcutol and ethanol migrate upon incorporation of the bulk vitamin. Hence the higher *gauche* conformation fraction and lower melting temperature are detected compared to those of the typical H_{II} structure.

The influence of the VE and VEA guest molecules and their location in the three H_{II} phases is illustrated in Figure 7. Introduction of the hydrophobic guest molecules, VE and VEA, led to their incorporation between the GMO tails, with vitamin E located closer to the interface (Figure 7). Both guest molecules, especially when replacing all TAG molecules, exhibited mainly interactions with the carbonyl and methylene groups and correspondingly delayed the GMO tail fusion temperature. It was suggested that integration of the Transcutol

or ethanol in the fluid H_{II} structure led to partial migration toward the hydrophobic region, thus their impact was less pronounced.

Conclusions

In this study, we correlated the solubilization capacity and solubilization loci of three types of reverse hexagonal liquid crystals to the nature of the solubilizates that were entrapped within their core and the interface. The combined data obtained from the three methods (SAXS, thermal behavior and FTIR) helped to clarify where these molecules are located once solubilized.

Ascorbic acid (AA) and ascorbyl palmitate (AP) represent two solubilizates, one very hydrophilic, promoting strong hydrogen bonding with the lipid headgroups, and the other composed of a hydrophilic head attached to a lipophilic tail. It was found that in the H_{II} structure, the ascorbic acid acts as a chaotropic guest molecule, localized in the water-rich core and at the interface. Hence, its effect is more pronounced on the water and interface behavior, including cylinder swelling, water fusion temperature and interactions with hydroxyls and carbonyl functional groups.

The AP is also a chaotropic guest molecule with its head located in the vicinity of the GMO headgroup while its tail is embedded close to the surfactant tail (solvated by it). AP affected all three regions in the mesophase—the water-rich core, the interface and the lipophilic-rich region. For instance, AP decreases water and tail fusion temperatures and interacts with the carbonyl and methylene groups.

It was revealed that as ethanol is incorporated, the H_{II} phase becomes more fluidic and AA or AP were solubilized more in the water than in the interface, while if Transcutol is embedded in the structure the solubilizates are located closer to the interface. In the typical system and in the presence of ethanol, the solubilizates' impact was more pronounced on the water behavior than on the interface and *vice versa* in the presence of Transcutol.

D-α-tocopherol and D-α-tocopherol acetate being lipophilic with relatively small hydratable hydrophilic groups and bulky lipophilic moieties are incorporated between the GMO tails. Vitamin E is located closer to the interface than the VEA. Both guest molecules, especially when replacing all TAG molecules, mainly exhibited interactions with the carbonyl and methylene groups and correspondingly delayed the GMO tail fusion temperature.

Supporting Information Available: Small-angle X-ray diffraction patterns of the (a) GMO/tricaprylin 90/10 mixture, representing the typical H_{II} systems and (b) GMO/(tricaprylin+Transcutol) 90/10 mixture, representing the fluids H_{II} systems, where all mixtures contained 12.5 wt % water and where the patterns were measured at 25 °C and the arrows on trace b indicate the locations of the [11] and [20] diffraction peaks. This material is available free of charge via the Internet at http://pubs.acs.org.

References and Notes

(1) Fahr, A.; van Hoogevest, P.; May, S.; Bergstrand, N.; Leigh, M. L. S. *Eur. J. Pharm. Sci.* **2005**, *26*, 251–265.
(2) Shan-Yang, L.; Hsiu-Li, L.; Mei-Jane, L. *Adsorption* **2002**, *8*, 197–202.
(3) Jensen, J. W.; Schutzbach, J. S. *Biochemistry* **1984**, *23*, 1115–1119.
(4) Ericsson, B.; Eriksson, P. O.; Löfroth, J. E.; Engström, S. Cubic phases as delivery system for peptide drugs. In *Polymeric Drug and Drug Delivery System*; American Chemical Society: Washington, DC, 1991; 251−265.
(5) Wallin, R.; Engström, S.; Mandenius, C. F. *Biocatalysis* **1993**, *8*, 73–80.
(6) Razumas, V.; Kanapienienė, J.; Nylander, T.; Engström, S.; Larsson, K. *Anal. Chim. Acta* **1994**, *289*, 155–162.
(7) Moaddel, T.; Friberg, S. E.; Brin, A. *Colloid Polym. Sci.* **1996**, *274*, 153–159.
(8) Nylander, T.; Mattisson, C.; Razumas, V.; Miezes, Y.; Håkansson, B. *Colloids Surf. A* **1996**, *114*, 311–320.
(9) Razumas, V.; Larsson, K.; Miezes, Y.; Nylander, T. *J. Phys. Chem.* **1996**, *100*, 11766–11774.
(10) Caboi, F.; Nylander, T.; Razumas, V.; Talaikyté, Z.; Monduzzi, M.; Larsson, K. *Langmuir* **1997**, *13*, 5476–5483.
(11) Banerjee, R. *J. Biomater. Appl.* **2001**, *16*, 3–21.
(12) Gregoriadis, G. *Trends. Biotechnol.* **1995**, *13*, 527–537.
(13) Amar-Yuli, I.; Wachtel, E.; Shalev, D. E.; Aserin, A.; Garti, N. *J. Phys. Chem. B* **2008**, *112*, 3971–3982.
(14) Zanoni, J. N.; Freitas, P. *Arq. Gastroenterol.* **2005**, *42*, 186–190.
(15) Peterkofsky, B *Am. J. Clin. Nutr.* **1991**, *54*, 1135S–1140S.
(16) May, J. M.; Qu, Z. C.; Cobb, C. E. *J. Free. Radic. Biol. Med.* **1996**, *21*, 471–480.
(17) Pokorski, M.; Marczak, M.; Dymecka, A.; Suchocki, P. *J. Biomed. Sci.* **2003**, *10*, 193–198.
(18) Burton, G. W.; Traber, M. G. *Annu. Rev. Nutr.* **1990**, *10*, 357–382.
(19) Bradford, A; Atkinson, J.; Fuller, N.; Rand, R. P. *J. Lipid Res.* **2003**, *44*, 1940–1945.
(20) Dong, Y. D.; Larson, I.; Hanley, T.; Boyd, B. J. *Langmuir* **2006**, *22*, 9512–9518.
(21) Granger, D. N.; Hernandez, L. A.; Grisham, M. B. *Viewpoints Dig. Dis.* **1986**, *18*, 13–17.
(22) Valcheva-Kuzmanova, S.; Krasnaliev, I.; Galunska, B.; Belcheva, A. *Autonomic Autacoid Pharmacol.* **2007**, *27*, 131–136.
(23) Lake, J. A. *Acta Crystallogr.* **1967**, *23*, 191–194.
(24) Amar-Yuli, I.; Wachtel, E.; Ben-Shoshan, E.; Danino, D.; Aserin, A.; Garti, N. *Langmuir* **2007**, *23*, 3637–3645.
(25) Amar-Yuli, I.; Wachtel, E.; Shalev, D. E.; Moshe, H.; Aserin, A.; Garti, N. *J. Phys. Chem. B* **2007**, *111*, 13544–13553.
(26) Hyde, S. T. In *Handbook of Applied Surface and Colloid Chemistry*, 1st ed.; Holmberg, K., Ed.; Wiley: New York, 2001; Chapter 16.
(27) Ivanova, R.; Lindman, B.; Alexandridis, P. *Langmuir* **2000**, *16*, 3660–3675.
(28) Koynova, R.; Brankov, J.; Tenchov, B *Eur. Biophys. J.* **1997**, *25*, 261–274.
(29) Tsvetkova, N.; Koynova, R.; Tsonev, L.; Quinn, P.; Tenchov, B. *Chem. Phys. Lipids* **1991**, *60*, 51–59.
(30) Saturni, L.; Rustichelli, F.; Di Gregorio, G. M.; Cordone, L.; Mariani, P. *Phys. Rev. E* **2001**, *64*, 040902/1–4.
(31) Nilsson, A.; Holmgren, A.; Lindblom, G. *Biochemistry* **1991**, *30*, 2126–2133.
(32) Sharp, K. A.; Madan, B.; Manas, E.; Vanderkooi, J. M. *J. Chem. Phys.* **2001**, *114*, 1791–1796.
(33) Nilsson, A.; Holmgren, A.; Lindblom, G. *Chem. Phys. Lipids* **1994**, *71*, 119–131.
(34) Holmgren, A.; Lindblom, G.; Johansson, L. B.-A. *J. Phys. Chem.* **1988**, *92*, 5639–5642.
(35) Inoue, T.; Matsuda, M.; Nibu, Y.; Misono, Y.; Suzuki, M. *Langmuir* **2001**, *17*, 1833–1840.

JP802737K